Open Access Article

# An observational study of air and water vapour convergence over the Bernese Alps, Switzerland, during summertime and the development of isolated thunderstorms

EDWARD GRAHAM[1,2], ERNEST N'DRI KOFFI[1,*] and CHRISTIAN MÄTZLER[1]

[1]Institute of Applied Physics, University of Bern, Sidlerstrasse 5, 3012 Bern, Switzerland
[2]Lews Castle College, University of the Highlands and Islands, Stornoway, HS2 0XR, Scotland

## Abstract

The daytime summer phenomenon of the mesoscale transport of air and water vapour from the Swiss lowlands into the nearby western Alps, leading to orographic convection, is investigated using a range of independent observations. These observations are: Global Positioning System (GPS) integrated water vapour (IWV) data, the TROWARA microwave radiometer, MeteoSwiss ANETZ surface weather station data, the Payerne radiosonde, synoptic analyses for Switzerland and Europe, EUMETSAT and NOAA visible and infra-red satellite images, MeteoSwiss operational precipitation radar, photographs and webcam images including time-lapse cloud animations. The intention was to show, using GPS IWV data, that significant differences in IWV may occur between the Swiss plain and nearby Alps during small single-cell Alpine thunderstorm events, and that these may be attributable to regional airflow convergence. Two particular case studies are presented for closer examination: 20 June 2005 and 13 June 2006. On both days, fine and warm weather was followed by isolated orographic convection over the Alps in the afternoon and evening, producing thunderstorms. The thunderstorms investigated were generally small, local, discrete and short-lived phenomena. They were selected for study because of almost stationary position over orography, rendering easy observation because they remained contained within a particular mountain region before dissipating. The results show that large transfers of air and water vapour occur from the Swiss plain to the mountains on such days, with up to a 50% increase in GPS IWV values at individual Alpine stations, coincident with strong airflow convergence in the same locality.

**Keywords:** airmass thunderstorms, air and water vapour convergence, Switzerland, mountain-plain air circulation system.

## 1 Introduction

One of the outstanding issues in meteorology today is a full description of the initiation, development and life cycle of a thunderstorm. Although there has been a considerable improvement in observational and modelling tools over recent decades, the forecasting and nowcasting of thunderstorms remain a considerable challenge, especially in relation to the initiation of convection (WECKWERTH and PARSONS, 2006; WILSON et al., 1998).

Thunderstorms can form and develop in any geographic location where there is significant thermal instability. Depending on the environment in which they develop (*e.g.* strong wind shear), they can become severe. Hence, they are responsible for the development of many severe weather phenomena, such as lightning, large hail, severe wind gusts, extreme precipitation and tornadoes.

There are four recognised types of thunderstorms: single-cell, multicell clusters, multicell lines, and supercells (HOUZE, 1993; MADDOX, 1980, and references therein).

The situations described in this paper are of the single-cell type. Such thunderstorms may occur during otherwise fine weather conditions; they comprise of one updraft core and may also be termed as "air-mass thunderstorms", forming as they do away from the boundaries of different airmasses. Despite this, the various factors that drive their life cycle still remain a challenge and in most cases it is quite difficult to have enough observational data that permit a meaningful description of the various stages of their life cycle.

Two of the main factors which lead to single-celled thunderstorms are a supply of moisture and low-level convergence. Surface moisture convergence generally precedes the triggering of thunderstorms by a few hours, and such convergence favours the transport of the surface humidity to higher levels, given sufficient atmospheric instability. Under favourable conditions, they may develop over any type of topography, but most often they occur over mountainous regions, as there is usually greater instability over orography than over neighbouring lowlands.

This study deals with a particular meteorological phenomenon that exists in Switzerland on fine summer days,

*Corresponding author: Ernest N'Dri Koffi, Institute of Applied Physics, University of Bern, Sidlerstrasse 5, 3012 Bern, Switzerland, e-mail: ernest.koffi@jrc.ec.europa.eu

namely the flow and convergence of air and water vapour from the Swiss plateau into the nearby mountains (the western Alps and the Jura), sometimes leading to the outbreak of isolated showers and single-cell thunderstorms. This phenomenon occurs quite frequently during the summer half of the year and is often repeated over several consecutive days when the surface synoptic pressure gradient is slack. It is usually associated with a mid-to-upper level ridge of high pressure stretching across south-west Europe and relatively weak windshear with height. Such conditions aid the development of local, thermally-driven diurnal wind systems between mountain and valley and between mountain and plain, which in turn have the ability to focus orographic convection into small, well-defined, discrete areas. Weak windshear usually induces short-lived storms which therefore remain almost stationary within a particular mountain area. Consequently, they can increase flood and torrent risk in the Alps, but these types of thunderstorms usually do not propagate onto the Swiss lowlands.

The diurnal transport of air from the boundary layer into higher parts of the troposphere by mountains on fine summer days is known by some authors as "*mountain venting*" and is an important process in the transport of boundary layer atmospheric pollutants into free troposphere (HENNE et al., 2004). In a study of a deep Alpine valley on the south side of the Alps (near Bellinzona; see Fig. 1a), the above authors conclude that three times the valley air mass is exported vertically per day in fair weather conditions. Meanwhile, HENNE et al. (2005), have also shown that convection over the Alps on selected fine summer days contributed to an increase up of 1.3 mm in the integrated water vapour content downwind of the Alps.

In this study, we will look at western Switzerland only, where the research for this work has been completed, although the results could easily be extrapolated to other mountainous regions. Following previous work by HUNTRIESER et al. (1997) and MOREL and SENESI (2002), and using common meteorological knowledge gained from living in the areas for several years, we concur that there appears to be two main preferred trigger points of orographic convection in western Switzerland, which are (see Fig. 1);

(i)  The Jura ridge, straddling the Swiss-French border, to the north of the Swiss plain.
(ii) The western Alps, from eastern shore of Lake Geneva, through the valley of Saanen, to Interlaken; referred to subsequently as the "Bernese Oberland" from now on in this study.

MOREL and SENESI (2002), in a study of large Mesoscale Convective Storms greater than 10,000 km$^2$ using METEOSAT infra-red satellite imagery, identified the region near Lake Neuchâtel (Fig. 1) as having one of the highest frequency of incidence of cold cloud thunderstorms (less than -45°C cloud top temperature) triggering north of the Alps (*i.e.* the place where cirrus thunderstorm anvils are first detected). However, we suggest here that the reason for this apparent maximum near Lake Neuchâtel is advection downwind of the thunderstorm cirrus anvils (on the prevailing westerly or northwesterly upper tropospheric jetstream) from the original source of convection located a few kilometres upwind within the Jura mountains themselves.

Meanwhile, in a study of severe thunderstorms for the whole of Switzerland, HUNTRIESER et al. (1997) state that most thunderstorms (66%) formed over western Switzerland, reaching mature stage further east over central Switzerland and in the Alpine foothills. The authors also state importantly that "*convective systems depend primarily on large-scale processes for developing a suitable thermodynamic structure, while mesoscale processes act mainly to initiate convection*", and "*topography plays a crucial role for the initiation of thunderstorms in a mountainous country like Switzerland*" - both statements are very relevant and applicable for this work.

In this study, the primary objective was to gain a better understanding of evolution of mesoscale airflow convergence and integrated water vapour patterns of small orographic Alpine thunderstorms. Furthermore, we intended to (i) determine the trends in total IWV mass within the area of orographic convection, and that (ii) significant differences in IWV may occur between the Swiss plain and nearby Alps on certain days, and these differences may be attributable to regional airflow convergence of boundary layer winds.

A wide range of observational systems has been used in this study, including Global Positioning System (GPS) IWV data, MeteoSwiss ANETZ weather station information and the TROWARA microwave radiometer time series. Because it was not possible to have observational data from both France and Switzerland for this study, it was decided to leave out the Jura region at this time, but concentrate solely on the area of the (ii) Bernese Oberland (western Alps), which is completely contained within the boundaries of all available Swiss observational systems.

To achieve our abovementioned objectives, we will initially describe the methodology used (section 2). In section 3, we make a detailed description of two selected case studies using various data sources. Conclusions and recommendations for further work are presented in section 4.

# 2    Data and methodology

## 2.1    Data

All data used in this study consist of independent observations, many of them from Swiss or European remotely sensed systems and networks. They are as follows: the Swiss receiving network of the Global Positioning
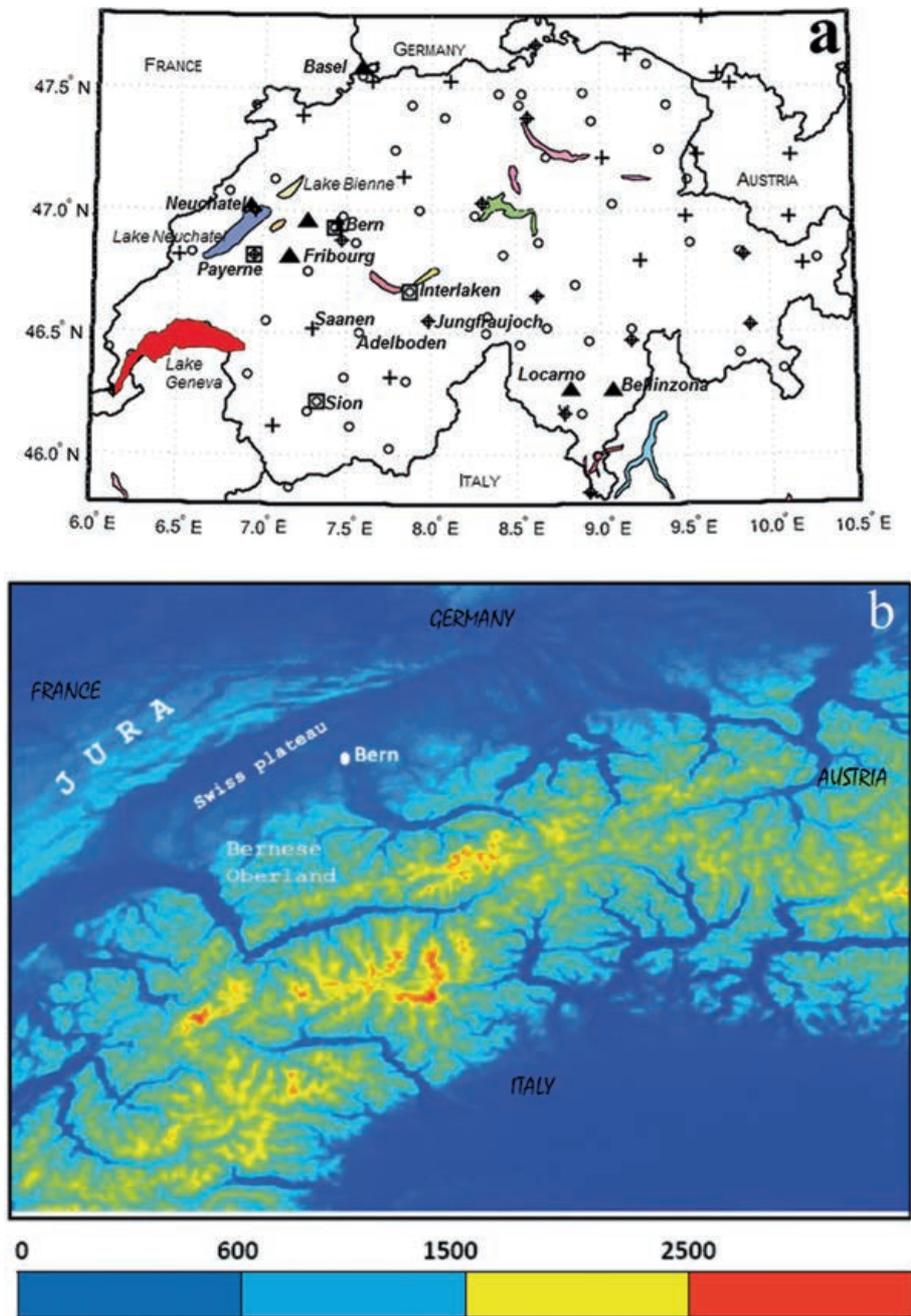
**Figure 1:** a) A map of Switzerland, showing international borders and placenames mentioned in the text. The locations of the 70 rain gauge stations of the MeteoSwiss ANETZ surface meteorological network are indicated by open circles. The locations of the 31 GPS measurement stations for integrated water vapour are shown by crosses. The four stations used to calculate the surface wind "Convergence/Divergence" are indicated by open squares (namely Bern, Payerne, Sion and Interlaken). b) The topography of western Switzerland (metres, see legend), as determined by the United States Geological Survey 1 km resolution digital terrain model (USGS, 1996). The location of the Jura mountain ridge, the Swiss plateau and the Bernese Oberland (a part of the northern Swiss Alps) are shown by text labels, as is the location of the city of Bern.

System (GPS) integrated water vapour (IWV) data, the TRoposperic WAter vapour Radiometer (TROWARA) microwave radiometer in Bern, MeteoSwiss Automatic Network (ANETZ) surface weather station data, the Payerne radiosonde, MeteoSwiss synoptic analyses for Switzerland and Europe, EUMETSAT Meteosat and National Oceanic and Atmospheric Administration (NOAA) visible and infra-red satellite images, Meteo-Swiss operational precipitation radar, private visual photographs, public webcam images and time-lapse cloud animations. Readers are referred to MORLAND and MÄTZLER (2007) and MÄTZLER and MORLAND (2009)

for further information about the GPS and TROWARA observing systems and their meteorological uses in Switzerland, respectively. The advantages and limitations of the MeteoSwiss operational precipitation radar product in a mountainous country like Switzerland are discussed in GERMANN et al. (2006). For the sake of brevity, only few examples of these various data sets are presented in this paper, and readers are referred to GRAHAM and KOFFI (2009) for further in-depth details. GRAHAM and KOFFI (2009) also discussed the limited applicability of using the Payerne radiosonde in deriving indices of the environments in which storms developed. Later, in section 3, we present the results of two particular case studies from the summers of 2005 and 2006, when isolated orographic convection developed over the Alps whilst conditions remained mostly fine, warm and sunny on the Swiss plateau.

## 2.2 Methodology

### 2.2.1 Computation of low level convergence/ divergence

Here, we developed a new method based on the use of surface winds observed by a conventional meteorological network (the MeteoSwiss ANETZ network) to quantify the convergence or divergence of airflow near the surface. Following the Boussinesq approximation, assuming constant air density (see HOLTON, 1994, for an overview), the continuity equation is reduced to the following expression:

$$\frac{\partial u}{\partial x} + \frac{\partial v}{\partial y} = -\frac{\partial w}{\partial z} \qquad \text{Eq. 1}$$

where $u$, $v$, and $w$ are the west-east, south-north, and vertical components of the winds (ms$^{-1}$) in the $x$, $y$, and $z$ directions, respectively. The convergence or divergence in the horizontal plane $Div_h$ is given by:

$$Div_h = \frac{\partial u}{\partial x} + \frac{\partial v}{\partial y} \qquad \text{Eq. 2}$$

Under the assumptions that vertical wind component is zero at the ground and that $Div_h$ is constant with respect to the vertical coordinate until a given level, the ascent of an air parcel (positive $w$ or a convergent flow*)* is depicted by a negative value of $Div_h$. Thus, the air is transported to an upper level by decreasing the area within which the initial air parel is contained. Conversely, a positive value of $Div_h$ value implies subsidence (negative $w$ or a divergent flow) of air from the higher levels to the surface, and thus the horizontal surface area of the air parcel increases. Overall, for a given air parcel contained within an area A (m$^2$), the rate at which A becomes greater (divergence) or smaller (convergence) over the time is $\frac{dA}{dt}(m^2/s)$. Thus,
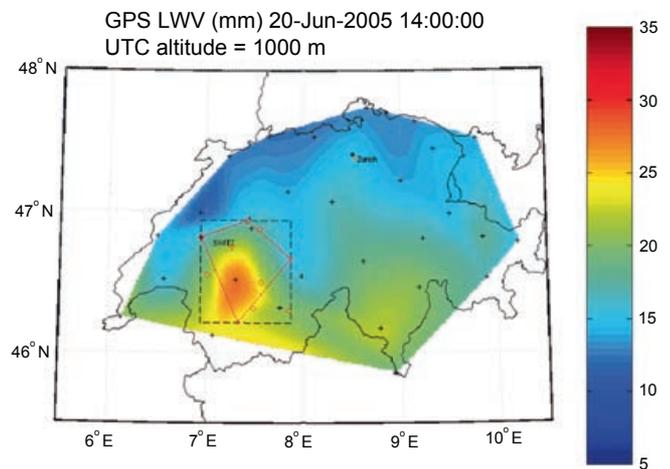


**Figure 2:** Global Positioning Satellite (GPS) integrated water vapour (mm) for 1400 UTC on 20 June 2005, corrected to a value of 1000 metres above sea level, using the successful scheme as described by MORLAND and MÄTZLER (2007). The dashed-line rectangular box marks the fixed area within which the total GPS integrated water vapour (kg) was calculated throughout the day, and which is plotted in Figs. 6(a) and 11(a). The (inner) red solid-line polygonal box marks the dynamic area within which the convergence was calculated using the MeteoSwiss ANETZ surface weather stations, which is plotted in Figs. 6(b) and 11(b); the locations of the ANETZ stations are marked by small open circles. The 31 GPS receiving stations across Switzerland are marked by crosses.

$Div_h$ (Eq. 2) can be expressed as a function of the the relative rate (s$^{-1}$) at which this area changes size as follows:

$$Div_h = \frac{1}{A} \cdot \frac{dA}{dt} = \frac{1}{A} \cdot \left[ \frac{A' - A}{t' - t} \right] \qquad \text{Eq. 3}$$

where an original area $A$ of an air parcel at time $t$ becomes a new area $A'$ at the time $t'$ a little later. In this particular study, convergence and divergence (Eq. 3) values were calculated using MeteoSwiss ANETZ wind data, for 10 and 30-minute time intervals, for the preselected areas within the Bernese Oberland in which orographic convection had taken place. Such an area is illustrated as the diamond-shaped polygonal box in Fig. 2. Here, the polygon is composed of four lines joining four different ANETZ stations, which surround the area of orographic convection. Wind data from each corner of the polygon (each ANETZ station) is then used to calculate the convergence (squeezing) or divergence (stretching) towards or away from this area through time, using the method described above. Thus, the size and shape of the box can vary during the day, according to the wind vectors at each ANETZ station.

A small difficulty arose when calculating $Div_h$ (Eq .3). This is because $Div_h$ is defined in the horizontal plane (see Eq. 2–Eq. 3), and calculations on an entirely flat level were not possible using the ANETZ data, due to

the complex orography in Switzerland. However, careful choice was made to select ANETZ stations in the same altitude range when calculating the convergence. These stations were on average 529 m with a standard deviation of 44 m above sea level, and were used to assess low-level boundary layer convergence (valley-bottom). Other groups of stations at higher altitudes were also chosen to represent mountain-level flow, but these were not used in this particular study and are therefore not presented here. As a result of this slight problem, $Div_h$ values calculated using this method will hereafter be referred to as "Convergence"/"Divergence" (contained within double quotations), but this difficulty is not thought to have any major effect on results. The uncertainties related to this issue are dependent on the vertical structure of $Div_h$ within the layer $529 \pm 44$ m above sea-level. Unfortunately, such a vertical profile is not available for this study, and would be very difficult to obtain given the complex orography of Switzerland.

### 2.2.2   Calculation of the Total Mass of IWV

The link between water vapour convergence and severe convection is well-known. DONE et al. (2005) showed that there is usually a slow increase of water vapour convergence during the hours before the onset of deep convection, followed by a rapid increase 20 to 40 minutes prior to the onset of severe convection. Using GPS IWV, CHAMPOLLION et al. (2004) monitored the evolution of a convective system associated with precipitation, from the water vapour accumulation stage through maturation of the convective cell, to the final decay of the system.

MORLAND et al. (2006) estimate an IWV error of 0.75 mm in a study using the fixed network of 31 GPS stations located across Switzerland. Meanwhile, HAGEMANN et al. (2003) estimate an accuracy of better than 0.7 mm, MATTOLI et al. (2005) estimating an accuracy in the range 0.75 to 1 mm. More recently, however, VAN BAELEN et al. (2011) state that the errors of GPS observations are 'difficult to estimate', quoting an error of 1 mm for elevations greater than 30° but up to 1.5 mm for elevations down to 5° (BENDER et al., 2008). These estimated errors represent about 10% of the total IWV variation seen on the two case study days to be examined in this paper.

We calculated the total mass of integrated water vapour (in kilograms) as a time series for each hour of the day, using the GPS IWV dataset, over approximately the same area for which the convergence was calculated. However, it was not possible to co-locate the exact boundaries of this GPS IWV box with the polygonal area used in the "convergence/divergence" calculations, because of latter box's dynamic nature. Therefore, a new larger static rectangular box was chosen for the calculation of the total IWV mass, but whose boundaries completely included the dynamic area of the "convergence" polygon at all times. This is allowed because

the storms under study were stationary. This is shown graphically in Fig. 2, where the dashed rectangular box marks the area within which the GPS IWV mass was calculated for each hour throughout the day (0.9° latitude/ longitude). The diamond-shaped polygon depicts the "convergence/divergence" area at 1400 UTC on this particular day.

The calculation of the GPS IWV mass within its given box was achieved as follows; (i) firstly, the individual GPS IWV station values (31 in total, marked by black crosses in Fig. 2) were corrected to a level of 1000 metres (an arbitrary height, chosen to represent the approximate mean height of the combined Bernese plain and mountains) using the same scheme as devised by MORLAND and Mätzler (2007), and (ii) secondly, the corrected IWV values were interpolated onto a "mesh grid" for the whole of Switzerland at a resolution at 0.02° latitude / longitude. This was obtained using the cubic interpolation function of the software Matlab (MATH WORKS, 1992). Finally, the corrected IWV mesh values were then summed for each pixel, and the given result of the total mass of IWV was calculated for the dashed rectangular box area, as shown in Fig. 6(a). This procedure was repeated for each hour of the day in question in order to obtain a time series.

### 2.2.3   Convective indices and Payerne soundings

Although the Payerne soundings (the only one launched in Switzerland) were found to have a limited applicability in deriving convective indices for this study (GRAHAM and KOFFI, 2009), the Convective Available Potential Energy (CAPE) and the Convective INhibition (CIN) energy have nevertheless been computed from Payerne sonde data, as these two indices are relevant for the initiation and development of storms. The CAPE represents the amount of buoyant energy available to accelerate a parcel vertically, while the CIN (a negative energy) determines the amount of energy that must be overcome to allow an air parcel to rise by its own accord to the level of free convection. Based on the indices developed for thunderstorms mainly in USA, a CAPE value of greater than 2500 J/kg indicates a very unstable atmosphere with possible severe weather. Further details can be found in *e.g.* EMANUAL (2004), HUNTRIESER et al. (1997), KOFFI et al. (2007), and the NOAA National Weather Service website (http://www.crh.noaa.gov/lmk/soo/docu/indices.php).

## 3   Applied case studies of (i) 20 June 2005 and (ii) 13 June 2006

In this section, we present two case studies using the methodology for wind "convergence"/"divergence" as derived in section 2.2.1, together with the associated water vapour convergence derived from GPS IWV data (section 2.2.2).

## 3.1 Case study of 20 June 2005

### 3.1.1 Weather pattern

The synoptic weather pattern over Europe on 20 June 2005 was dominated at mid-to-upper tropospheric levels by a strong ridge of high pressure stretching northwards over western Europe, bringing warm and mostly stable conditions. Switzerland lay in a gentle northerly flow of air on the eastern flank of this ridge, but surface pressure gradients were largely slack over central Europe. In the absence of frontal boundaries, this location is usually considered as an unlikely place for the formation of severe or widespread thunderstorms. There was a marked north-south surface moisture gradient across the Alps, with a dewpoint of only around 10°C over Germany, but around 20 to 22°C in northern Italy. Incursion of moist air into the southern Alps may therefore have been possible due to prevailing southerly winds in northern Italy and mountain venting on the south side of the Alps. Further details can be found in GRAHAM and KOFFI (2009).

Surface air temperatures rose rapidly from 11°C or 12°C near dawn to over 30°C across the Swiss plateau during the late afternoon, peaking at 31.5°C at Basel-Binningen weather station in the north of Switzerland. This large diurnal range in air temperature ranges indicates near-maximum insolation, a dry atmosphere (allowing maximum infra-red radiation), and a shallow inversion. All MeteoSwiss ANETZ stations (as reported in MeteoSwiss' *Tageswetter* daily summary for 20 June 2005) recorded between 10 and 15 hours of bright sunshine during the day (but with the notable exception of the measurement station at Adelboden in the Bernese Oberland, which recorded 9.4 hours; see Fig. 1 for location). This strong sunshine, rapidly rising temperatures, weak surface pressure gradient, and weak windshear gave rise to near-ideal conditions for the development of local mountain-valley wind systems across Switzerland from mid-morning onwards, eventually leading to isolated convergence and near-stationary, temporary orographic convection.

It is estimated that a surface temperature of at least 35°C at Payerne would have been necessary to saturate a surface parcel and rise it through the depth of the troposphere (assuming no mixing); such high surface temperatures were unlikely on this day. However, as already discussed in GRAHAM and KOFFI (2009), it is important to state that the Payerne radiosonde data may be representative of conditions only on the Swiss plateau and therefore may be different from a sonde profile taken in the Alps at the same time. Bearing this in mind, the CAPE and CIN were calculated for 20 June 2005 using the sonde data for 12 UTC. The results confirmed strong stability with little chance of deep convection ocurring, with all values remaining below the threshold for severe storm development. The total CAPE value was 33 J/kg, which is a very low value. Similarly, the calculated value of -238 *J/kg* for CIN is not usually overcome by even the strongest convection. Yet, despite these forecasts, a single-cell thunderstorm with locally heavy precipitation did develop for a few hours that evening over the Bernese Oberland.

### 3.1.2 Bern EXWI and TROWARA Data

Data from the University of Bern Exact Sciences (EXWI) building roof-top instruments of TROWARA and EXWI weather station for 20 June 2005 were also analysed (Figs. 3 and 4). The location of Bern EXWI is indicated in Fig. 1. The weather data (Fig. 3) shows a near-sinusoidal profile of air temperature. No clouds were observed during the whole day by an infra-red camera, which is also confirmed by the zero trace of integrated liquid water [ILW] content calculated from the TROWARA data. A slight dip in the absolute humidity occurred near 1800 UTC. The TROWARA IWV trace (also Fig. 3) shows a change to higher variability from about 1300 UTC onwards (co-incident with onset of convection in nearby mountains), with a sudden drop near 1500 UTC (Fig. 3; co-incident with the commencement of deep convection over the Alps). This drop is perhaps reminiscent of traces of the onset of the sea-breeze (a density current) in the British Isles (*e.g.* SIMPSON, 1994). Whilst there is no sea in Switzerland, like the sea-breeze a mountain-plain air circulation system is also an air ascent-descent circulation system caused by pressure differences, and thus the presence of such cannot be ruled-out.

Meanwhile, Fig. 4 shows the absolute time derivative of TROWARA IWV for 20 June 2005. There are clearly large absolute rates of change of IWV between 1200 and 1800 UTC, with the maximum around 1500 UTC. These indicate changes in the depth of the boundary layer over Bern on this afternoon (MÄTZLER and MORLAND, 2009).

### 3.1.3 Development of Thunderstorms over Jura and Bernese Oberland

Analyses of satellite and webcam imagery reveal that large towers of cumulus congestus convection began at favoured orographic points over the Swiss Jura and over the Bernese Oberland from 1300 UTC (3 pm local time) to 1800 UTC, quickly dying out thereafter (see Fig. 1 for locations). The thunderstorms were not at all exceptional by Swiss standards, but because of their isolated nature they can be easily identified as discrete mesoscale phenomena using high resolution satellite imagery. Apart from these instances, there were no other cases of convection across the whole of Switzerland on this day, and skies remained largely clear – thus, the areas of convection remained very well defined, small scale and therefore relatively easy to monitor.

Fig. 5 shows the images from three different observational systems at approximately the same time (1500-
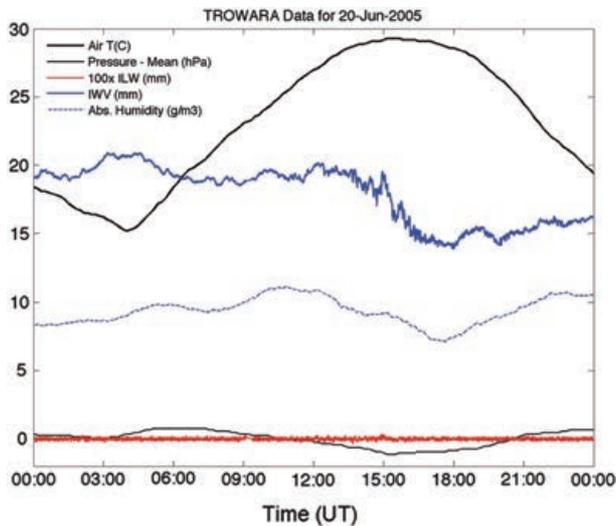
**Figure 3:** The Tropospheric microwave Water Vapour Radiometer (TROWARA) and University of Bern Exact Sciences (EXWI) rooftop weather station data for 20 June 2005. Data is depicted as follows: Thick black line = air temperature (°C); Thick blue line = integrated water vapour (IWV, mm); dotted blue line = absolute humidity (g/m$^3$); red = integrated liquid water (ILW multiplied by 100, mm); thin grey line = surface pressure fluctuations around the mean pressure during the day (hPa). Please see MÄTZLER and MORLAND (2009) for the IWV and ILW refined algorithms.
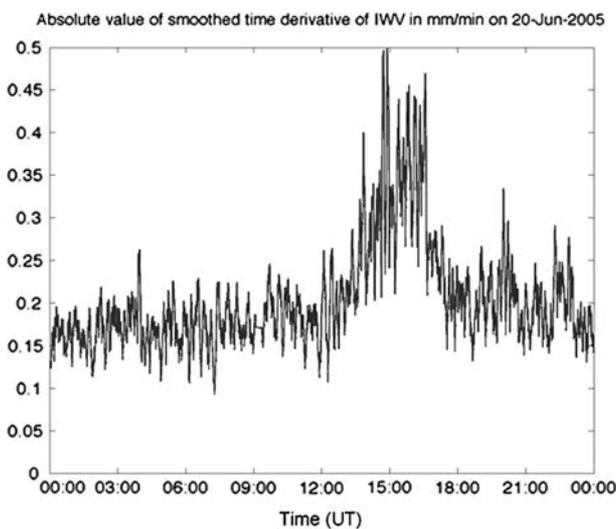


**Figure 4:** Absolute value of smoothed time derivative of TROWARA IWV (mm/min) on 20 June 2005, calculated using TROWARA microwave radiometer.

1530 UTC) on this afternoon of 20 June 2005. Fig. 5(a) comprises of a Meteosat High Resolution Visible 1km image of Switzerland; Fig. 5(b) a visible photograph of the thunderstorm looking south from Fribourg, Switzerland (see Fig. 1 for locations); and Fig. 5(c) a MeteoSwiss precipitation radar image. When combined with the GPS IWV image shown in Fig. 2 (1400UTC, 60-90 minutes earlier), these four images capture well

the meteorological situation on this afternoon. Note the co-incidence of features between all four independent observational images, particularly the sharp precipitation boundary and IWV gradients near the source of the convective towers, but fanning more gently southwards under the thunderstorm cirrus anvil. Note also the deep blue sky devoid of smaller clouds in the photograph in Fig. 5(b), indicating a dry atmosphere (probably due to low relative humidity preventing growth of hydroscopic aerosols which restrict visibility) and possible descent of air near the observer's location.

Moreover, a six-hourly time sequence of co-incidental satellite and GPS IWV images from 1300 to 1900 UTC was inspected (GRAHAM and KOFFI, 2009). In summary, the GPS IWV images show a remarkable concentration of water vapour features over the Saanen GPS station (location Fig. 1) in the Bernese Oberland (up to 50%, or ~10 mm, greater than at nearby stations) from 1300 UTC onwards, with general higher IWV values south of the Alps at all times.

### 3.1.4  Discussion of Convergence / Divergence and Total Mass of IWV Results

Fig. 6(a) presents the time series of total GPS IWV mass (kg) for the Bernese Oberland area, corrected to a level of 1000 metres by following the same method as described by MORLAND and MÄTZLER (2007). The total IWV mass values rise from about $1.1 \times 10^{11}$ kg (110 megatons) during the early morning to nearly $1.3 \times 10^{11}$ kg during the time of maximum orographic convection in mid-afternoon. This represents a 18% increase in total IWV within the selected area, although an individual station increase of nearly 50% (~10 mm IWV) occurred at Saanen GPS station in the centre of the Bernese Oberland, as already stated. The maximum IWV mass values co-incide well with the timing of maximum extent of the thunderstorm development and anvil (GRAHAM and KOFFI, 2009).

Meanwhile, the "convergence/divergence" values in Fig. 6(b) show a steady decrease (convergence) during the morning, steepening by early afternoon during the time of maximum convection (strong convergence), in agreement with results of DONE et al. (2005). A sudden switch to divergence (positive) values occurs at 1400 UTC, considerably earlier than might be expected, when considering the evolution of the satellite, GPS images and Fig. 6(a). However, Fig. 6(d) shows that this sudden switch is co-incidental with a precipitation event (*i.e.* downdraught divergence) that occurred at Sion ANETZ station, which may explain the sudden switch to divergence in Fig. 6(b). This mismatch between the "convergence" (Fig. 6b) and GPS IWV (Fig. 6a) could also be due to (i) limitations of our method where the shape of the dynamic "convergence" box differs from the non-dynamic shape of the GPS IWV box; (ii) the choice of ANETZ weather stations, which may be too widely-spaced data for our method on this occasion,
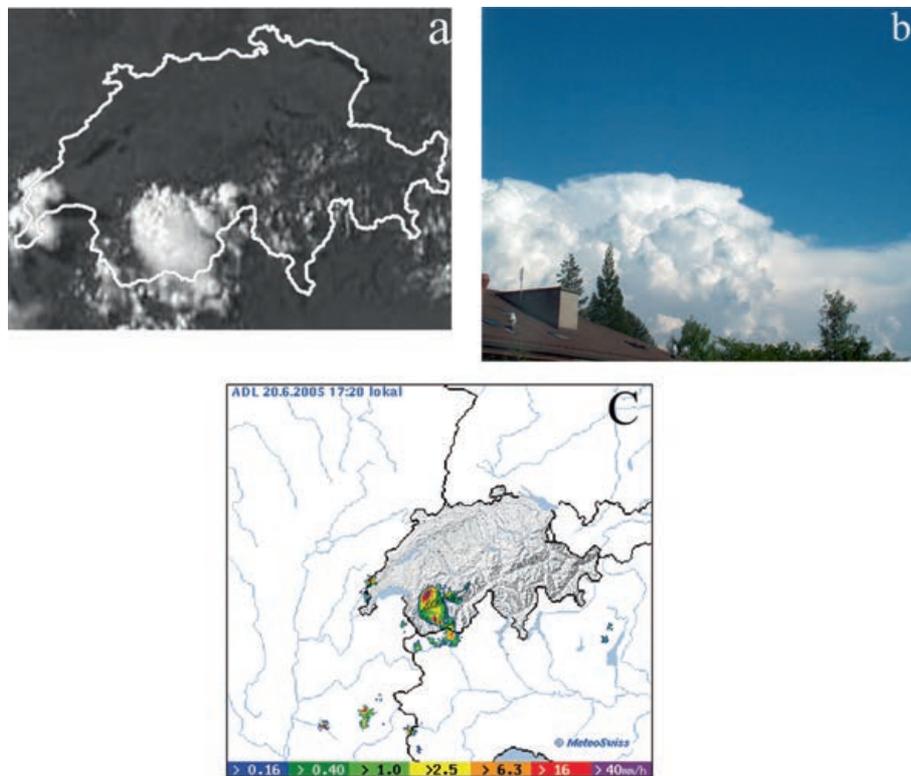
**Figure 5: (a)** Meteosat Second Generation High Resolution Visible (MSG HRV) 1 km image of Switzerland on 20 June 2005 at 1527 UTC (image kindly provided by EUMETSAT); **(b)** Visible photograph looking south from Fribourg, Switzerland at 1515 UTC on same day (photograph by EDWARD GRAHAM); **(c)** MeteoSwiss precipitation radar at 1520 UTC (image kindly provided by MeteoSwiss). These three images can be compared with Fig. 2 which shows the Global Positioning System (GPS) integrated water vapour for Switzerland at 1400 UTC on the same afternoon.

and (iii) airflow at different levels. In the case of (i), our method relies on the dynamic nature of the "convergence" box, so this limitation cannot be eliminated. Accounting for (ii) and (iii) is beyond the scope of this paper, but could feasibly be dealt with in a very high resolution field and modelling campaign such as *e.g.* COPS (WULFMEYER *et al.*, 2011).

Note, however, the occurrence of Cloud-to-Ground (CG) lightning (Fig. 6[c]) just after the time of maximum convergence and during the period of greatest water vapour concentration. Note also the IWV total mass starts to decrease (Fig. 6a) when the precipitation occurs (*i.e.* loss, Fig. 6d), when divergence occurs (*i.e.* downdraughts, Fig. 6b) and when the peak in lightning activity subsides (*i.e.* less convection, keeping droplets or ice bouyant, Fig. 6c).

Our "convergence/divergence" calculations (Fig. 6b) are in agreement with the findings of COOPER et al. (1982). The authors described five main stages in the temporal variations of the divergence derived from surface wind observations during deep convective activity, namely (i) the beginning of persistent convergence which occurred here around 1000 UTC, (ii) the peak of the convergence (at about 1200 UTC in our case), (iii) the change from convergence to divergence (inflection point), (iv) the peak divergence coinciding with the max-

imum of the CG lightning flashes, and (iv) the end of the cycle and thunderstorm decay.

## 3.2 Case study of 13 June 2006

### 3.2.1 Weather pattern

The synoptic weather pattern over Europe on 13 June 2006 was again dominated by a strong ridge of high pressure over western Europe, bringing warm and stable conditions to Switzerland (GRAHAM and KOFFI, 2009). Again, like in the first case study, surface pressure gradients were very slack, thus giving favourable conditions for the development of mesoscale thermal wind systems during the day.

The Payerne radiosonde launched at 12 UTC (GRAHAM and KOFFI, 2009) showed a mostly dry and stable atmosphere with 19.0 mm of total integrated water vapour and a stable inversion at 3400 metres. It is estimated that surface temperatures of at least 35°C would be necessary to initiate deep convection to the tropopause, which was very unlikely on this day, as maximum air temperatures were expected to reach only around 30°C. Thermodynamic indices again showed little potential for severe thunderstorms, with computed CAPE and CIN values to be 1.9 J/kg and -220 J/kg, respectively.
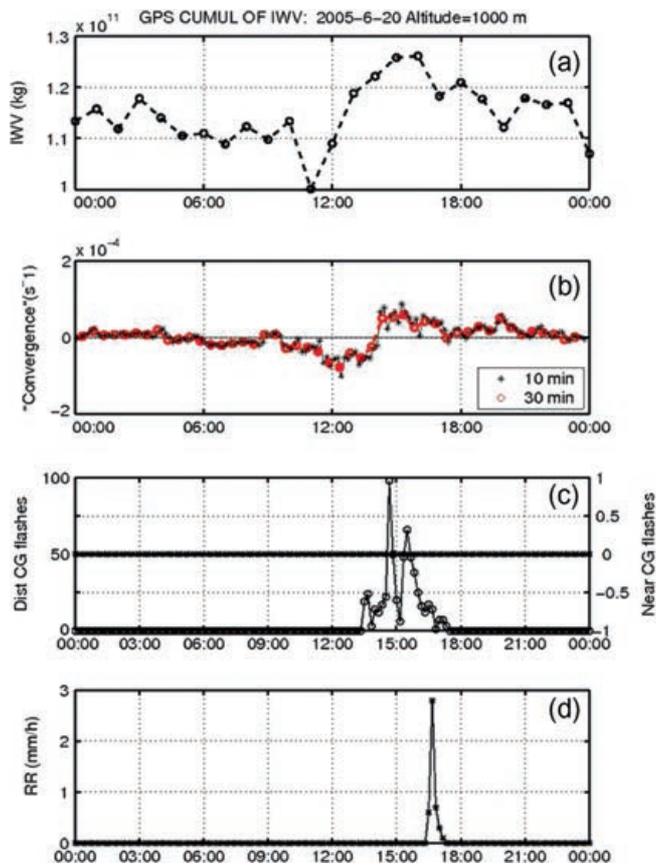
Figure 6: a): Time series of total GPS integrated water vapour (IWV) mass (kg) for the area marked within the dashed-line black rectangle in Fig. 2, corrected to a level of 1000 metres (using the same method as described by MORLAND and MÄTZLER, 2007) from 0000 to 2400 UTC on 20 June 2005. b): "Divergence / Convergence" $(s^{-1})$ for the same period for the area marked within the solid-line red polygon in Fig. 2, as calculated using the four nearest MeteoSwiss ANETZ weather station 10-minute (red circles and thick dashed red line) and 30-minute (black asterix and thin solid black line) wind vector data. Values below zero indicate that convergence is taking place, values above zero values indicate that divergence is occurring, within the designated area. c): Number of distant (3-30 km; circles) and near (0-3 km; stars with scale on the right side) Cloud-to-Ground (CG) lightning strikes recorded by the ANETZ weather stations within each 10-minute time period. d): Mean precipitation rate (mm/hr) for the same ANETZ weather stations located within the box for the same time period.

There was also little windshear with height, further indicating that the environmental conditions were poor for the generation of any severe thunderstorms. However, as discussed earlier and in GRAHAM and KOFFI (2009), the Payerne sonde data may have limited applicability for this work.

The possible role of gravity waves set off by cumulonimbus towers to initiate further convection in the near vicinity was investigated by retrieving webcam images at regular frequency through the internet. The animated results (not shown) suggest that propagating gravity waves are important in the development of individual convection surges, and on a separate occasion (24 June
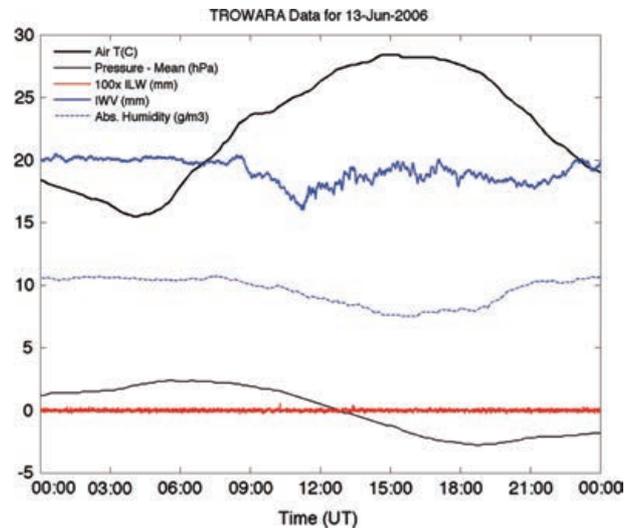
2005) a travelling gravity wave was visibly seen from Fribourg, Switzerland (GRAHAM and KOFFI, 2009).

### 3.2.2  EXWI weather station and TROWARA daily plots

The roof-top EXWI weather station and the TROWARA microwave radiometer at the University of Bern (Fig. 7 and further details in GRAHAM and KOFFI, 2009) showed that sunshine remained unbroken throughout the day, with a near sinusoidal profile of air temperature recorded.

Of particular interest in Fig. 7 is the TROWARA IWV trace, which shows much greater variability between ~0900 and ~1800 UTC, with lower-than-average values during the afternoon following a sharp dip around midday. These higher frequency daytime oscillations maybe related to convective surges in the boundary layer, but could possibly be manifestations of a mountain-plain air circulation system between the Alps and the Swiss lowlands. The authors here note that such early afternoon sudden "jumps" and increase in IWV variability are fairly regular occurrences during the summer in Bern.

Fig. 8 shows the absolute values of temporal rate of change of IWV for 13 June 2006, calculated using TROWARA microwave radiometer data (MÄTZLER and MORLAND, 2009). The values oscillate around 0.2 mm/min with a relatively sharp increase at around 1200 UTC with further maxima until 1400UTC. The timing of these maxima are coincident with the time of
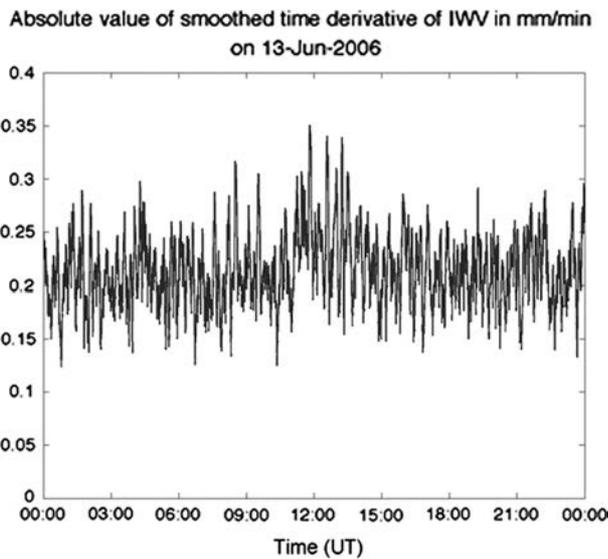


Figure 7: The Tropospheric microwave Water Vapour Radiometer (TROWARA) and University of Bern Exact Sciences (EXWI) rooftop weather station data for 13 June 2006. Data is depicted as follows: Thick black line = air temperature (°C); Thick blue line = integrated water vapour (IWV, mm); dotted blue line = absolute humidity (g/m³); red = integrated liquid water (ILW multiplied by 100, mm); thin grey line = surface pressure fluctuations around the mean pressure during the day (hPa). Please see MÄTZLER and MORLAND (2009) for the IWV and ILW refined algorithms.

**Figure 8:** Absolute value of smoothed time derivative of TROW-ARA IWV (mm/min) on 13 June 2006, calculated using TROW-ARA microwave radiometer.
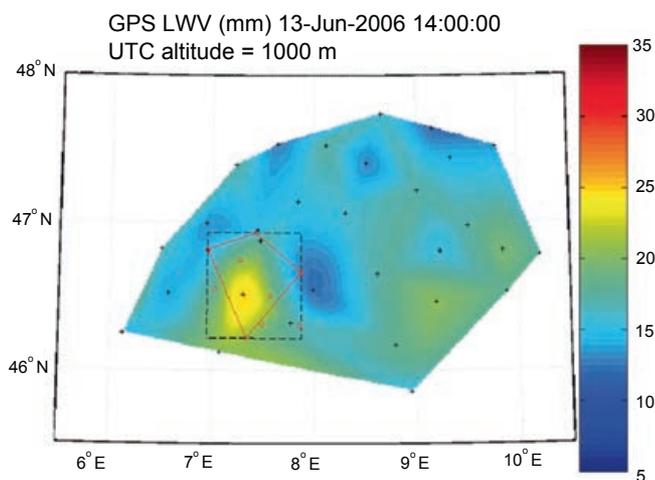


**Figure 9:** Global Positioning Satellite (GPS) integrated water vapour (mm) for 1400 UTC on 13 June 2006, corrected to a value of 1000 metres above sea level, using the successful scheme as described by MORLAND and MÄTZLER (2007). The dashed-line rectangular box marks the fixed area within which the total GPS integrated water vapour (kg) was calculated throughout the day, and which is plotted in Figs. 6(a) and 11(a). The (inner) red solid-line polygonal box marks the dynamic area within which the convergence was calculated using the MeteoSwiss ANETZ surface weather stations, which is plotted in Figs. 6(b) and 11(b); the locations of the ANETZ stations are marked by small open circles. The 31 GPS receiving stations across Switzerland are marked by crosses. A large positive anomaly is apparent surrounding Saanen GPS station (marked by the cross in the middle of the yellow colours). This was associated with orographic convection in the vicinity at the same time (see text for more details).

maximum water vapour convergence over the Bernese Oberland on this day (Fig. 11a).

### 3.2.3  GPS integrated water vapour maps

Similar to Fig. 2, Fig. 9 presents a colour map of the GPS IWV of Switzerland, corrected to a level of 1000 metres as performed in MORLAND and MÄTZLER (2007), for 1400 UTC on 13 June 2006. It can be seen that most stations on the northern Swiss plain have corrected IWV values of between 10 and 15 mm, but Alpine and southern stations have values 15 to 20 mm (with the exception of Jungfraujoch, 3584 metres, which was still above a dry inversion, identified earlier from the radiosonde, at 3400 metres). The greatest positive anomaly (25 mm) occurs again at Saanen GPS receiving station in the Bernese Oberland. This station is again located directly beneath the area where the strongest orographic convection took place on this day. Local showers and isolated thunderstorms broke out in this area around 1800 UTC in the evening (four hours later). This GPS IWV map, combined with that presented earlier in Fig. 2, clearly demonstrate the case that mesoscale differences in water vapour can occur due to orographic effects on warm summer days in Switzerland.

Meanwhile, Fig. 10 presents (a) a webcam image from Neuchatel looking south towards the Bernese Alps at 1800UTC, and (b) a precipitation radar image 30 minutes later at 1830UTC, on 13 June 2006. These two images can be compared with the GPS IWV image in Fig. 9 for 1400UTC on the same day (four hours earlier). The moderately-sized cumulonimbus cloud seen in the distance in Fig. 10(a) is subsequent to bright precipitation radar echoes over the Saanen region of the Alps 30 minutes later in the radar image in Fig. 10(b), but has been consequent of positive GPS IWV anomalies in the same region for up to the previous four hours (Fig. 9).

### 3.2.4  Total IWV mass and surface convergence over Bernese Oberland

Fig. 11(a) presents the time series of the total mass of GPS IWV, calculated for the same 0.9° latitude/longitude box, for the whole day of 13 June 2006. Like Fig. 6, it is again corrected to a level of 1000 metres as described in MORLAND and MÄTZLER (2007). The main feature of this graph is the slow, steady increase of IWV mass through the morning, followed by a sudden rise between 1200 and 1300 UTC, with a decrease later in the afternoon, especially around 2000–2100 UTC.

It can be seen from Fig. 11(b) that strong convergence (negative values) takes place within the selected area at around the same time (1200-1300 UTC) as the IWV mass increases (Fig. 11a), followed by a steady change towards divergent conditions (precipitation and outflow) by 1800 UTC. This plot therefore supports the hypothesis that meso-scale convergence of water vapour was initiated by orographic effects, followed by evening precipitation, divergence and outflow.
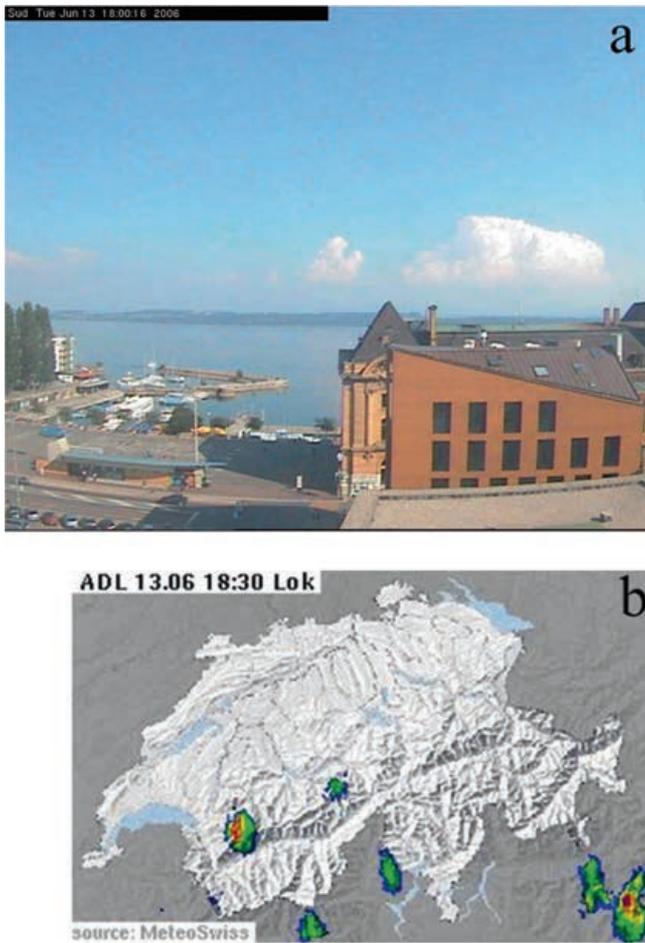
**Figure 10:** (a) Webcam image looking south from Neuchatel lakeside towards the Western Alps at 1800 UTC on 13 June 2006 (image courtesy of Neuchâtel police); (b) MeteoSwiss precipitation radar image at 1830 UTC. These images can be compared with Fig. 9 which shows the GPS IWV (mm) map for Switzerland four hours earlier at 1400 UTC on the same day.



**Figure 11:** As Fig. 6, but for 13 June 2006. No precipitation was recorded at any ANETZ rain gauges (panel *[d]*), but operational radar images (see Fig. 10*[b]*) suggested some fell in the vicinity.



**Figure 12:** Time series of GPS IWV (mm) at Saanen (SAAN, black solid line) and Payerne (PAYE, blue dashed line) for 13 June 2006. Note the strong anti-correlation between the two series during the afternoon.

Fig. 11(c) presents the number of CG lightning strikes recorded by the nearest ANETZ weather stations within each 10-minute time period. The first CG lightning strikes were recorded about two hours after the maximum IWV mass gain and around the time of maximum convergence, which is (more than) sufficient time for the cloud to grow into a precipitating system or thunderstorm. Lastly, Fig. 11(d) shows that no precipitation was recorded at any ANETZ rain gauges, but operational radar images (Fig. 10b) suggested some fell in the vicinity.

Meanwhile, the possible indication that a mountain-plain air circulation system may have occurred on 13 June 2006 is provided by Fig. 12, which shows hourly values of GPS IWV at Saanen and Payerne GPS receiving stations for the same day. There appears to be strong anti-correlation between the two curves during the afternoon, which could be caused by a moist ascending arm of convection above Saanen, and a corresponding drier, descending arm over Payerne. Evidence for the occur-
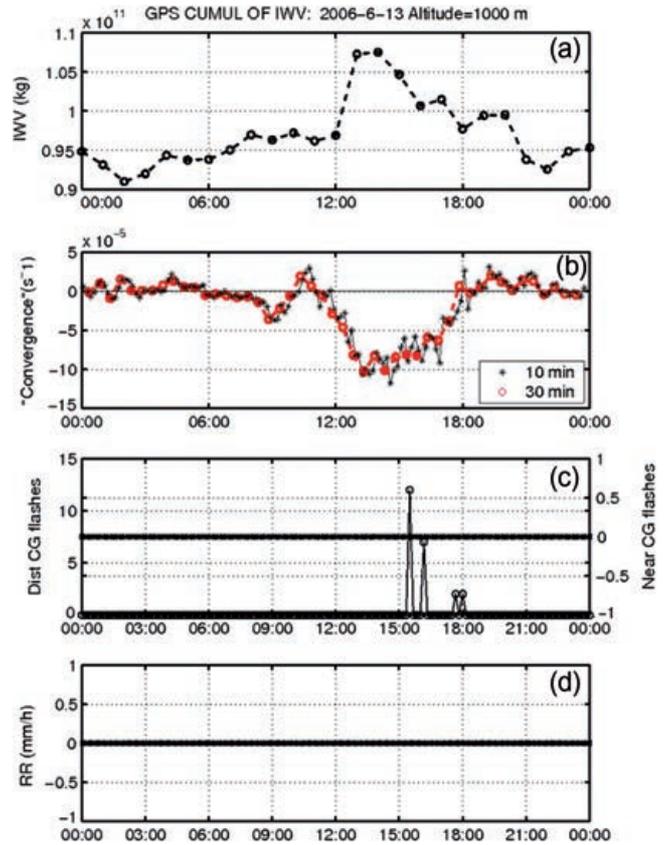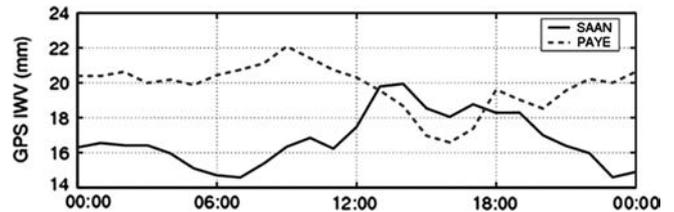
rence of such could be obtained through the use of local radiosonde launches, wind profilers or mesoscale meteorological modelling studies.

Finally, the computed rate of change (kg/hour) and power (kġ/hour) of the total IWV mass show a relatively constant rate of change until the afternoon between 1200 and 1300 UTC, when a sudden increase occurs (initiation of strong convergence) followed by gentler decreases (divergence, storm outflow) later in the afternoon and evening (GRAHAM and KOFFI, 2009). DONE et al. (2005) mentioned lead times of 20 to 40 minutes between the sudden increase in convergence and onset of severe

thunderstorms; in this case, our lead time is about 3 hours, if we consider the time difference between the peak in rate of change of IWV and peak in CG lightning strikes). The fact that deep convection initiation was marginal on this day and the thunderstorms were not severe probably accounts for some of this relatively long delay.

Interestingly, the two case studies examined in this paper bear some resemblances to those studied and discussed by HAGEN et al. (2011) and WULFMEYER et al. (2011) during the Convective and Orographically-induced Precipitation Study (COPS) in southern Germany in 2007. As discussed in HAGEN et al. (2011), small precipitation convective cells developed alternately over an orographic ridge, or to the lee side of the ridge. It was found that preferred cell initiation location depended strongly on the Froude number and tropospheric wind profile. WULFMEYER et al. (2011) refer to COPS Intensive Observation Period (IOP) 8b of 15 July 2007, when a single convective cell developed east of a mountain crest, and was favoured by the development of local circulation system and high insolation. In our two case studies presented here, although we had a much smaller amount of observational data available than during COPS, the type of cells analysed would appear to belong to "ridge" category of HAGEN et al. (2011), though more data and analyses would be needed to confirm this.

## 4    Conclusions

The case of mesoscale transport of air and water vapour from the Swiss lowlands into the Alps on summer days, associated with orographic convection and convergence, has been investigated in detail for two specific case studies during the summers of 2005 and 2006. A large range of observational data were used, including GPS integrated water vapour (IWV) data, TROWARA microwave radiometer data, ANETZ surface weather station data, satellite images, operational precipitation radar images, photographs, webcam images and time-lapse cloud animations. Two new methods of study were employed, namely:

(i) A new method to calculate the convergence of airflow over time at different orographic levels using surface weather station data was presented, yielding successful results.
(ii) A new method to calculate the amount and change of total mass of integrated water vapour over time for a specific mesoscale area (in this case, the Bernese Oberland) using the GPS IWV data was also presented, also with successful results.

The usefulness of the GPS IWV maps has been demonstrated alongside other independent mesoscale observational systems, such as satellite imagery, precipitation radar and photography; they can easily identify water

vapour anomalies associated with mesoscale cloud-precipitation systems, and they indicate that large positive GPS water vapour anomalies may precede thunderstorm occurrence by several hours. In our two case studies, individual GPS station IWV values increased by up to 50% (> ~10 mm) on days of strong orographic convection.

Changes in the total mass of IWV over the Bernese Oberland appear to be strongly related to surface convergence on fine summer days. Surface orographic convergence and IWV mass gain increase slowly during the morning, followed by sudden increases close to when the first outbreak of deep convection occurs, followed by more general divergence and outflow later in the evening. Good meteorological agreement between total mass of IWV, surface convergence, incidence of lightning and precipitation events has been demonstrated for our two case studies.

Apparent anti-correlation of the GPS IWV series between Payerne and Saanen suggests that there may be a mountain-plain (ascent-descent) air circulation system in operation between the Swiss plain and the Bernese Oberland, and curious features in the IWV trace of the TROWARA radiometer on fine summer days in Bern also suggest this, although more research is needed. Penultimately, thermodynamic indices calculated using the Payerne sonde data have limited applicability in the Alps during times of marginal thunderstorm forecasting, as indicated earlier by GRAHAM and KOFFI (2009).

Finally, it was also found that webcam images, when animated into movie loops, are an extremely useful method of remote observation, sometimes yielding new information on the character of clouds and thunderstorms, and their potential should not be underestimated compared to other observational techniques.

## 5    Recommendations for further work

Ultimately, high resolution model data (e.g. from the MeteoSwiss operational model) could provide new and further insight into the results of our study, particularly for airflow at higher levels of the atmosphere. Direct observation of a mountain-valley air ascent-descent system could be achieved by using a combination of remote sensing instruments, such as microwave radiometers, wind profilers, radar, multiple radiosonde or through very high resolution meteorological modelling. It is therefore recommended that these provide the focus for future work on this topic. Furthermore, it would be worthwhile to undertake a study of TROWARA IWV data for similar summer days to investigate the characteristics of the mid-day-early afternoon "jumps" in IWV above Bern. The GPS convergence method could be improved to include the possibility of tracking larger storms as they move and grow across Switzerland. If so, then the complete cycle of a Mesoscale Convective System (MCS) might be possible. Such a scheme could be developed using European-wide GPS data.

In addition to the useful GPS IWV data, this study proposes a new methodology on the quantification of wind convergence/divergence from surface wind observations. These two sources of data can complement the effort of EUMETSAT in stimulating meteorologists by using satellite images for nowcasting purposes. Indeed, within the EUMETSAT nowcasting Satellite Facilities Application (SAF) programme, a method capable to identify and track cloud shields from satellite images has been developed (MOREL and SENESI, 2002). Our methodology is beneficial to nowcasters that use this system, since our method is able to detect as early as possible the development of a subsequent cloud to be tracked.

## Acknowledgments

## References

BENDER, M., G. DICK, J. WICKERT, T. SCHMIDT, S. SONG, G. GENDT, M. GE, M. ROTHACHER, 2008: Validation of GPS slant delays using water vapour radiometers and weather models. – Meteorol. Z. **17**, 807–812.

CHAMPOLLION, C., F. MASSON, J. VAN BAELEN, A. WALPERSDORF, J. CHÉRY, E. DOERFLINGER, 2004: GPS monitoring of the tropospheric water vapor distribution and variation during the 9 September 2002 torrential precipitation episode in the Cévennes (southern France). – J. Geophys. Res. **109**, D24102, DOI: 10.1029/2004JD004897.

COOPER, H. J., M. GARSTANG, J. SIMPSON, 1982: The diurnal interaction between convection and peninsular-scale forcing over south Florida. – Mon. Wea. Rev. **110**, 486–503.

DONE, J.M., X.Y. HUANG, Y.H KUO, 2005: Investigating the relationship between water vapour convergence and severe convection using the WRF model at 1km resolution. – 11th Conference on Mesoscale Processes, American Meteorological Society, Albuquerque, New Mexico, USA.

EMANUEL, K.A. , 1994: Atmospheric Convection. Oxford University Press, 592 p.

GERMANN, U. G. GALLI, M. BOSCACCI, M. BOLLIGER, 2006: Radar precipitation measurement in a mountainous region. – Quart. J. Roy. Meteor. Soc. **132**, 1669–1692.

GRAHAM, E., E. KOFFI, 2009: An observational study of air and water vapour convergence over the western Alps

during summer and the development of isolated thunderstorms. – IAP Research Report, No. 2009-01-MW, Institut für angewandte Physik, Universität Bern. Available at: http://www.iap.unibe.ch/publications/publication.php. Other details can be found from here: http://www.iapmw.unibe.ch/research/projects/thunderstorms/gps_storms.html

HAGEN, M., J. VAN BAELEN, E. RICHARD, 2011: Influence of the wind profile on the initiation of convection in mountainousterrain. Quart. J. Roy. Meteor. Soc., **137** (S1), pp. 224–235. Doi:10.1002/qj.784

HAGEMANN, S., L. BENGTSSON, G. GENDT, 2003: On the determination of atmospheric water vapour from GPS measurements. – J. Geophys. Res. **108**, 4678.

HENNE, S., M. FURGER, S. NYEKI, M. STEINBACHER, B. NEININGER, S. F. J. de WEKKER, J. DOMMEN, N. SPICHTINGER, A. STOHL, A. S. H. PRÉVÔT, 2004: Quantification of topographic venting of boundary layer air to the free troposphere. – Atmos. Chem. Phys. **4**, 497–509.

HENNE, S., M. FURGER, A. S. F. PRÉVÔT, 2005: Climatology of Mountain Venting – Induced Elevated Moisture Layers in the Lee of the Alps. – J. Appl. Meteor. **44**, 620–633.

HOLTON, J.R., 1994: An Introduction to Dynamic Meteorology. – Academic Press, 511 p.

HOUZE, R.A., 1993: Cloud Dynamics. – San Diego and Oxford, UK, Academic Press  573 p.

HUNTRIESER, H., H. H. SCHIESSER, W. SCHMID, A. WALDVOGEL, 1997: Comparison of traditional and newly developed thunderstorm indices for Switzerland. – Wea. Forecast. **12**, 108–125.

KOFFI, E., M. SCHNEEBELI, E. BROCARD, C. MÄTZLER, 2007: The Use of Radiometer Derived Convective Indices in Thunderstorm Nowcasting. – IAP Research Report, No. 2007-02-MW, Institut für angewandte Physik, Universität Bern.

MADDOX, R. A., 1980: Mesoscale convective complexes. – Bull. Amer. Meteor. Soc. **61**, 1374–1387.

MATH WORKS, 1992: Matlab User's Guide, Natick, MA.

MÄTZLER, C., J. MORLAND, 2009: Refined Physical Retrieval of Integrated Water Vapour and Cloud Liquid for Microwave Radiometer Data. – IEEE Transactions Geosci. Remote Sens. **47**, 1585–1594.

MATTOLI, V., E. R. WESTWATER, S. I. GUTMAN, V. R. MORRIS, 2005: Forward model studies of water vapour using scanning radiometers during the Cloudiness Intercomparison Experiment. – IEEE Trans. Geosci. Remote Sens. **43**, 1012–1021.

MOREL, C., S. SENESI, 2002: A climatology of mesoscale convective systems over Europe using satellite infrared imagery. II: Characteristics of European mesoscale convective systems. – Quart. J. Roy. Meteor. Soc. **128**, 1973–1995.

MORLAND, J., C. MÄTZLER, 2007: Spatial Interpolation of GPS integrated water vapour measurements made in the Swiss Alps. – Meteor. Appl. **14**, 15–26.

MORLAND, J., M.A. LINIGER, H. HUNZ, I. BALIN, S. NYEKI, C. MATZLER, N. KAMPFER, 2006: Comparison of GPS and ERA40 IWV in the Alpine region, including correction of

GPS observations at Jungfraujoch (3584m). – J. Geophys. Res. **111**, D4102, 12 pp.

SIMPSON, J.E., 1994: Sea Breeze and local winds. – Cambridge University Press.

Van BAELEN, J., M. REVERDY, F. TRIDON, L. LABBOUZ, G. DICK, M. BENDER, M. HAGEN, 2011: On the relationship between water vapour field evolution and the life cycle of precipitation systems. – Quart. J. Roy. Meteor. Soc. **137**, 204–233.

WECKWERTH, T. M., D. B. PARSONS, 2006: A Review of Convection Initiation and Motivation for IHOP_2002. – Mon. Wea. Rev. **134**, 5–22, DOI: 10.1175/MWR3067.1.

WECKWERTH, T. M., J. W. WILSON, M. HAGEN, T. J. EMERSON, J. O. PINTO, D. L. RIFE, L. GREBE, 2011: Radar climatology of the COPS region. – Q. J. Roy. Meteor. Soc. **137**, 31–41.

WILSON, J. W., N. A. CROOK, C. K. MUELLER, J. SUN, M. DIXON, 1998: Nowcasting Thunderstorms: A Status Report. – Bull. Amer. Meteor. Soc. **79**, 2079–2099.

WULFMEYER, V., A. BEHRENDT, C. KOTTMEIER, U. CORSMEIER, C. BARTHLOTT, G. C. CRAIG, M. HAGEN, D. ALTHAUSEN, F. AOSHIMA, M. ARPAGAUS, H.-S. BAUER, L. BENNETT, A. BLYTH, C. BRANDAU, C. CHAMPOLLION, S. CREWELL, G. DICK, P. DI GIROLAMO, M. DORNINGER, Y. DUFOURNET, R. EIGENMANN, R. ENGELMANN, C. FLAMANT, T. FOKEN, T. GORGAS, M. GRZESCHIK, J. HANDWERKER, C. HAUCK, H. HÖLLER, W. JUNKERMANN, N. KALTHOFF, C. KIEMLE, S. KLINK, M. KÖNIG, L. KRAUSS, C. N. LONG, F. MADONNA, S. MOBBS, B. NEININGER, S. PAL, G. PETERS, G. PIGEON, E. RICHARD, M. W. ROTACH, H. RUSSCHENBERG, T. SCHWI-TALLA, V. SMITH, R. STEINACKER, J. TRENTMANN, D. D. TURNER, J. van BAELEN, S. VOGT, H. VOLKERT, T. WECKWERTH, H. WERNLI, A. WIESER, M. WIRTH, 2011: The Convective and Orographically-induced Precipitation Study (COPS): the scientific strategy, the field phase, and research highlights. – Q. J. Roy. Meteor. Soc. **137**, 3–30.